analytical chemistry

Article

pubs.acs.org/ac

Activity-Based DNA-Gold Nanoparticle Probe as Colorimetric Biosensor for DNA Methyltransferase/Glycosylase Assay

Zhan Wu, Zhen-Kun Wu, Hao Tang, Li-Juan Tang, and Jian-Hui Jiang*

State Key Laboratory of Chemo/Bio-Sensing and Chemometrics, College of Chemistry and Chemical Engineering, Hunan University, Changsha 410082, P. R. China

Supporting Information

ABSTRACT: We have developed a novel biosensor platform for colorimetric detection of active DNA methyltransferase/glycosylase based on terminal protection of the DNA-gold nanoparticle (AuNP) probes by mechanistically covalent trapping of target enzymes. This biosensor relied on covalent capture of target enzymes by activity-based DNA probes which created terminal protection of the DNA probes tethered on AuNPs from degradation by Exo I and III. This biosensor has the advantages of having highly sensitive, rapid, and convenient detection due to its use of the homogeneous assay format and strong surface plasmon absorption. Because the activity-based probes (ABPs) are mechanistically specific to target enzymes, this strategy also offers improved selectivity and can achieve the information about both abundance and activity of the enzymes. We have demonstrated this strategy using a human DNA (cytosine-5) methyltransferase (Dnmt 1) and a human 8-oxoguanine glycosylase (hOGG 1). The results reveal that the colorimetric response increases dynamically with increasing activity of the enzymes, implying a great potential of this strategy for DNA methyltransferase/glycosylase detection and molecular diagnostics and drug screening. Our strategy can also be used as a promising and convenient approach for visualized screening of ABPs for DNA modifying enzymes.

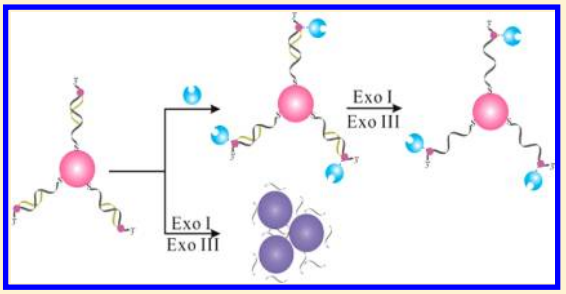

DNA methylation and repair are vital to the regulation of gene expression and the maintainence of genomic integrity and thus to normal functioning and survival of any living organism.[1,2] Recent evidence has revealed that DNA methylation and repair play crucial roles in dynamic epigenetic reprogramming of gene patterns that alter chromatin structures.[3,4] Both methylation and repair of DNA is accurately controlled by certain DNA modifiying enzymes such as DNA methyltransferases and glycosylases. Aberrant expression of DNA methyltransferases and glycosylases has profound implications in many important diseases such as cancers, Huntington's disease, and psychiatric disorders.[5,6] Therefore, the activities of DNA methyltransferases and glycosylases have become significant biomarkers for these diseases, and activity assay and inhibitor screening for these enzymes represent a valuable strategy to clinical diagnostics and therapeutics.[7,8]

Many existing methods for activity detection of DNA methyltransferases or glycosylases rely on a coupled assay for indirect quantification of the substrates or the products that are consumed or produced in the enzymatic processes.[9−13] For examples, a restriction endonuclease reaction which specifically cleaves methylated DNA is coupled in the activity assay for a DNA adenine methylation (Dam) methyltransferase.[9,10] Because the particular recognition site of this endonuclease does not match the substrate sequence CG for human methyltransferases as DNA cytosine-5 methyltransferases (DNMTs), this method is not suitable for human methyltransferase assay. Alternatively, a restriction endonuclease that is blocked by CpG methylation can be coupled to DNA methylation, which allows the detection of human DNA methyltransferases.[11] Another approach to the human DNA methyltransferase assay is to couple certain immunoassays to the DNA methylation reaction by the use of certain antibodies or binding proteins specific to methylated DNA.[12,13] This approach is usually time-consuming and technically demanding. Despite the wide use of these indirect methods, the enzyme activity thus determined is typically measured using the substrate amount processed by the enzymes. It, therefore, does not provide a direct assessment of the expression levels of active enzymes that are essential for elucidating their regulation states. An additional problem is that the enzymatic products or substrates coexisting in complex biological samples will interfere with the coupled assay. Hence, there is a constant need for the methods that allow sensitive, selective, and convenient quantification of active DNA methyltransferases and glycosylases.

Activity-based probes (ABPs) are a quickly evolving technology ideally suited for the analysis of enzyme activity.[14−16] An ABP is a molecule consisting of a properly positioned reactive site for covalent conjugation with the target enzyme and a tag for visualization or separation of the covalently bound enzyme. ABPs represent a useful tool for chemical proteomics and have been successfully developed for

Received: December 10, 2012
Accepted: April 2, 2013

   dx.doi.org/10.1021/ac303575f | *Anal. Chem.* XXXX, XXX, XXX−XXX

discovery of enzyme targets, interpretation of enzyme mechanism, identification of substrate selectivity, and elucidation of activity site architecture.[17−19] Despite such impressive progresses, ABPs for DNA modifying enzymes including methyltransferases and glycosylases have been largely unexplored.[20,21] In order to identify particular DNA modifying enzymes and gain insight into their functions, new analytical strategies for development of ABPs and detection of enzyme activity are necessary.

Here, we report the proof-of-principle of a novel ABP-based colorimetric biosensor strategy for detecting DNA methyltransferase/glycosylase activity. This biosensor relies on covalent capture of target enzymes by activity-based DNA probes, which creates terminal protection of the DNA probes from degradation by exonucleases.[22,23] This strategy is demonstrated using two model systems, a human DNA (cytosine-5) methyltransferase (Dnmt 1) and a human 8-oxoguanine glycosylase (hOGG 1). It is known that Dnmt 1 has a central role in the complex epigenetic regulatory network controlling gene expression in mammalian cells,[24] while hOGG 1 is responsible for repairing one of the most abundant oxidatively modified lesions 8-hydroxy-2-deoxyguanosine (8-OH-dG).[25] Because covalent trapping of target enzymes by their ABPs is mechanistically specific and quantitatively correlated to the active enzymes, this biosensor can offer very high selectivity and achieve the information about both abundance and activity of the enzymes. With the use of a gold nanoparticle-based colorimetric assay, the developed strategy can create a convenient platform for visualized detection of enzyme activity and screening of ABPs for these enzymes with high sensitivity and selectivity.

EXPERIMENTAL SECTION

Reagents and Materials. Klenow fragmemt (3′ exo-), human DNA (cytosine-5) methyltransferase (Dnmt 1), human 8-oxoguanine-DNA glycosylase (hOGG 1), exonuclease I (Exo I), and exonuclease III (Exo III) were purchased from New England Biolabs (Ipswich, MA, USA). 5-Aza-2′-deoxy-cytidine-5′-triphosphate (5-Aza-dCTP) was purchased from MoBiTec (Göttingen, Germany). Sodium cyanoborohydride was from Sigma Aldrich. MicroSpin G-50 column was purchased from GE Healthcare (Amersham, USA). Other reagents were obtained from Sinopharm Chemical Reagent Co. Ltd. (Shanghai, China). All solutions were prepared using ultrapure water, which was obtained through a Millipore Milli-Q water purification system (Billerica, MA, USA) and had an electric resistance >18.3 MΩ. The oligonucleotides used in this work were synthesized from Takara Biotechnology Co. Ltd. (Dalian, China). Thermodynamic parameters and secondary structures of all oligonucleotides were calculated using bioinformatics software (http://www.bioin-fo.rpi.edu/applications/). The sequences of the synthesized single-stranded oligonucleotides were given in Table S1 (Supporting Information), and the doubled-stranded oligonucleotides were given in Table S2 (Supporting Information).

Synthesis of DNA ABPs for Dnmt 1. Oligonucleotide DNA Sequences **1** and **2** (250 pmol) were hybridized in 10 mM Tris−HCl (pH, 7.9) buffer containing 10 mM $MgCl_2$, 50 mM KCl, and 1 mM dithiothreitol by heating to 90 °C for 5 min and slowly cooling to room temperature. Upon addition of 0.08 u/μL Klenow fragment (3′-5′-exo), dTTP, dGTP, and dATP at 1 mM final concentration, and either 5-aza-dCTP or dCTP at 1 mM, the Sequence **1** was extended to produce either containing 5-aza-dC Sequence **3** or Sequence **4** at 37 °C for 6 h at final volume of 50 μL. dTTP, dGTP, dATP, and dCTP or 5-aza-dCTP were eliminated using a MicroSpin G-50 column that had been equilibrated with ultrapure water for 1 min.

Preparation of DNA-Modified Gold Nanoparticle (AuNPs). AuNPs were prepared by citrate reduction of $HAuCl_4$ according to a reported protocol.[26] The nanoparticles were characterized by TEM (JEOL-1230, JEOL Co. Ltd. Japan) and appeared to be nearly monodisperse with an average diameter of 13 nm. The concentration of these AuNPs was determined to be 3.3 nM based on the extinction coefficient of 2.7×10^8 M^{-1} cm^{-1} at 520 nm for 13 nm AuNPs using a UV−visible absorption spectrometer (UV 2450, Shimadzu, Japan).

AuNPs were modified with thiol-labeled DNA oligonucleotides according to a documented procedure.[27] Briefly, 2 mL of aforementioned citrate-capped AuNPs was concentrated to 100 μL via centrifugation at 20 000g for 10 min. The 5′-thiol-modified oligonucleotides (500 μL, 2 μM) were added to the concentrated AuNP solution (100 μL, ∼66 nM) accompanied with shaking for 1 min. After reaction for 24 h at room temperature, two aliquots of 80 μL of phosphate buffer (PB, pH 7.4, 100 mM) and 35 μL of phosphate buffer salt (PBS, pH 7.4, 10 mM) containing 2 M NaCl were separately added into the AuNP solution with 0.1 M NaCl final concentration for 48 h and finally salted to 0.3 M NaCl for 24 h. The unmodified oligonucleotides were removed by centrifugation at 20 000*g* for 15 min followed by resuspension of the sediment in 2 mL of Tris−HCl buffer (10 nM Tris−HCl, 50 mM NaCl, 1 mM EDTA, pH 8.0). This step was repeated three times to completely remove excessive thiol-labeled oligoncleotides. Then, the DNA-modified AuNPs were redispersed in 600 μL of Tris−HCl buffer (10 mM Tris−HCl, 50 mM NaCl, 1 mM EDTA, pH 8.0) and stored at 4 °C until use. The final concentration of DNA-modified AuNPs is ∼33 nM, not considering the loss of AuNPs during the preparation process. The number of DNA strands per nanoparticle was determined to be ∼76 according to a procedure reported previously using a FITC-labeled sequence.[28] That is, the surface coverage of DNA probe is $\sim 1.59 \times 10^{13}$ stands/cm^2.

Preparation of Activity-Based DNA-Gold Nanoparticle Probe. The sufficient complementary DNA strand was mixed with DNA modified AuNPs (10 μL, ∼33 nM) in Dnmt 1 assay buffer (50 mM Tris−HCl, 1 mM EDTA, 50 mM NaCl, pH 7.8) or in hOGG 1 assay buffer (10 mM Tris−HCl, 50 mM NaCl, 10 mM $MgCl_2$, pH 7.9) separately. The mixtures were heated to 90 °C and incubated for 2 min followed by slow cooling to room temperature (over ∼4 h). The superfluous complementary DNA strand can be not removed.

Activity Analysis of Dnmt1/hOGG 1. For quantitative determination of Dnmt 1, a series of standard Dnmt 1 solutions and ∼3.3 nM activity-based DNA-gold nanoparticle probe were incubated at 37 °C for 90 min to allow sufficiently trapping in 50 μL assay buffer supplemented with 100 ng/μL BSA and 160 μM *S*-adenosyl-L-methionine (SAM). Then, 5 mM $MgCl_2$, 0.4 U/μL Exo I and 2 U/μL Exo III were added.

For quantitative determination of hOGG 1, an activity-based DNA-gold nanoparticle probe with a concentration of ∼3.3 nM was resuspended in 50 μL of assay buffer supplemented with 100 ng/μL BSA and a series of standard hOGG 1 solutions along with 100 mM $NaBH_3CN$; the reaction was performed at 37 °C for 90 min to allow sufficiently binding. Then, the resulting mixture was heated to 90 °C for 5 min prior to adding 0.4 U/μL Exo I and 2 U/μL Exo III. The digestion reaction in

dx.doi.org/10.1021/ac303575f | *Anal. Chem.* XXXX, XXX, XXX−XXX

the each system was monitored by a UV/vis absorption spectrometer (Shimadzu UV-2450, Kyoto, Japan) or directly visualized with naked eyes. The absorption measurements were performed at room temperature in a 50 μL quartz cuvette.

Characterization Experiments. The gel electrophoresis assays were performed under the conditions as mentioned above but with the following changes: 1 μM ABP probe of Dnmt 1 and hOGG 1; 104 U/mL of Dnmt1 and 256 U/mL of hOGG 1. After the digestion by Exo I and Exo III, the resulting solutions were heated to 85 °C for 10 min to terminate the reaction followed by adding 1 μM respective complementary DNA strand to permit complete hybridization.

The gel electrophoresis was conducted using the DNA sample (10 μL per well) on a 3% aragose gel with a fluorescence stain ethidium bromide (0.5 μg/mL) in 50 mM Tris−borate running buffer (pH 9.2) containing 2 mM EDTA at 100 V for 2 h. After electrophoresis, the gel was visualized via fluorescence detection using a Tocan 240 gel imaging system (Shanghai Tocan Biotechnology Company).

The hydrodynamic sizes of DNA-modified AuNPs and the AuNPs aggregates were determined by dynamic light scattering using a Malvern Zetasizer 3000 HS particle size analyzer (Malvern Instruments, Worcs, UK). Transmission electron microscopy (TEM) was also used to characterize the sizes of the DNA-modified AuNPs and the AuNPs aggregates. Samples were prepared by dropping the solution of 5 μL onto a carbon-coated copper grid. The solution was clicked from the edge of the grid with a piece of filter paper after 1 min. TEM images were obtained from a Hitachi TEM JEOL-1230 (Japan).

RESULTS AND DISCUSSION

Analytical Principle of ABP-Based Colorimetric Biosensor for Dnmt 1/hOGG 1. Our biosensor was based on covalent capture of target enzymes such as DNA methyltransferase Dnmt 1 or glycosylase hOGG 1 by activity-based DNA probe. This approach created terminal protection of the DNA probes from degradation by exonucleases I and III (Exo I and III). Figure 1 illustrates the general principle of the ABP-based colorimetric biosensor for Dnmt 1 or hOGG 1. Gold nanoparticles (AuNPs) were decorated with the double-stranded ABP DNA probe that contained an enzyme-reactive nucleotide (5-aza-dC or 8-oxo-dG) and a thiol modifier at 5′ terminus in one of the two strands. Because the negatively charged DNA probes displayed strong eletrostatic repulsion between each other, the ABP-decorated AuNPs can exhibit excellent stability and dispersion in the solution. When the ABP-decorated AuNPs were incubated with Exo I and III, the DNA probes would be stepwisely degraded from the 3′ end. Hence, the eletrostatic repulsion between AuNPs would be alleviated, which would destabilize AuNPs into large aggregates with a concomitant red-to-purple color change of the solution. In contrast, in the presence of target enzyme such as Dnmt 1 or hOGG 1, ABPs were subjected to attack by active enzymes at the reactive sites, forming a covalent DNA−protein complex via different mechanisms. Specifically, Dnmt 1 was covalently trapped at the C6 position of the 5-aza-C base ring in the ABP because the absence of a proton at the N5 position prevented β elimination (Figure 1B), while hOGG 1 was irreversibly captured at the C1 position of the lesion base 8-oxo-G in the ABP because the hydrolisis of a Schiff base intermediate was intercepted by the reducing agent $NaBH_3CN$ (Figure 1C). The trapped enzyme protein created terminal protection for the ABP DNA from digestion by Exo I and III,[22,23] which

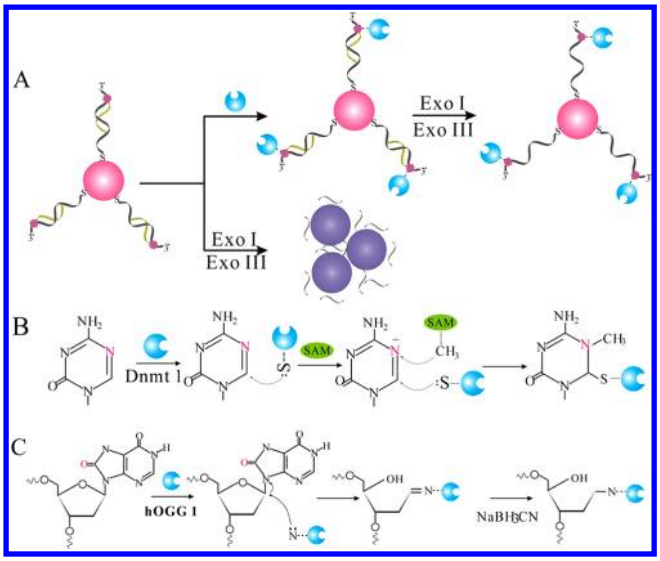

Figure 1. (A) Schematic representation of the ABP-based colorimetric biosensor strategy. (B) Trapping mechanism of Dnmt 1. A covalent complex forms between the sulfhydryl group of cysteine in the Pro-Cys motif of Dnmt1 and the C6 position of 5-aza-dC base ring followed by the transfer of a methyl group from SAM to the N5 position, where the absence of a proton prevents β elimination and thus causes trapping of Dnmt 1. (C) Trapping mechanism of hOGG 1. hOGG 1 utilizes an enzyme-borne nitrogen (Lys 249) nucleophile to displace the lesion base 8-oxo-dG by attack at C1. Rearrangement of the initial covalent intermediate yields a Schiff base intermediate, which ordinarily proceeds hydrolysis to liberate the enzyme but can be intercepted by the reducing agent $NaBH_3CN$, leading to irreversible trapping of hOGG 1 on the ABP.

maintained the dispersion of AuNPs in the solution with the color remaining unchanged. As a result, the surface plasmon absorption of AuNPs was dynamically dependent upon the amount of active enzymes, allowing qualitative and quantitative detection of the enzyme activity.

It is noteworthy that the developed ABP-based biosensor strategy had several advantages over traditional methods because covalent trapping of target enzymes by their ABPs was mechanistically specific and quantitatively correlated to the active enzymes. It allowed simultaneously detection of enzyme activity and abundance with high selectivity. Additionally, due to its homogeneous assay format and the sensitivity of surface plasmon absorption, this strategy can offer improved reproducibility, increased sensitivity, and simplified operation and enable the potential for high-throughput automation. Moreover, it created a much more useful and convenient approach for visualized screening of ABPs for DNA modifying enzymes, which was conventionally tackled by time-consuming gel electrophoresis analysis. In addition, it was reported that DNA-modified gold nanoparticles remained very stable and kept monodispersity in complicated biological media such as sera and cell extracts.[29,30] The resistance of DNA-modified gold nanoparticles to nucleases present in biological media was also demonstrated.[27,31] As a result, because of the specificity of covalent trapping of target enzymes by the activity-based probes, our method will not be affected by coexisting proteins, avoiding possible false negative signals in the assays of real biological samples.

Activity Assay of Dnmt1 Using ABP-Based Colorimetric Biosensor. The ABP DNA probe **1** which contained a 5′-aza-dC at hemimethylated CpG site was obtained via

dx.doi.org/10.1021/ac303575f | Anal. Chem. XXXX, XXX, XXX−XXX

hybridization of Sequence **2** and Sequence **3**. Figure 2 depicts typical absorption spectral responses of the biosensing strategy

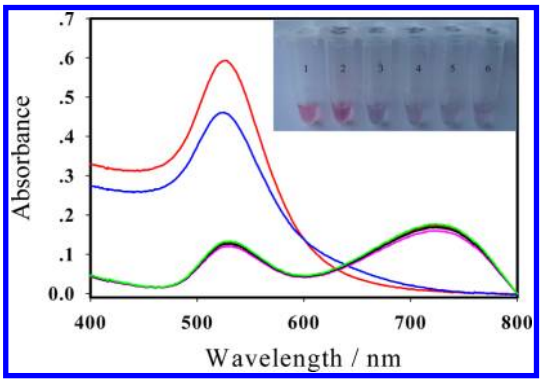

Figure 2. Typical absorption spectra obtained in assays of Dnmt 1. ABP probe **1** modified AuNPs before (red, tube 1) and after (green, tube 3) digesion by 0.4 U/μL Exo I and 2 U/μL Exo III; adding 104 U/mL Dnmt 1 into ABP probe 1 modified AuNP system followed by digestion with 0.4 U/μL Exo I and 2 U/μL Exo III (blue, tube 2); adding 104 U/mL Dnmt 1 into control probe **1** modified AuNP system followed by digestion with 0.4 U/μL Exo I and 2 U/μL Exo III (black, tube 4); adding 104 U/mL Dnmt 1 into control probe **2** modified AuNP system followed by digestion with 0.4 U/μL Exo I and 2 U/μL Exo III (pink, tube 5); adding 1 mM inhibitor of Dnmt 1 and 104 U Dnmt 1 into ABP probe 1 modified AuNP system followed by digestion with 0.4 U/μL Exo I and 2 U/μL Exo III (dark red, tube 6). The insets are the photographs for the corresponding systems.

in the activity assay of Dnmt 1. AuNPs decorated with ABP DNA probe 1 were well dispersed in aqueous solution, displaying a red color with a single surface plasmon absorption peak centered at 526 nm in Dnmt 1 assay buffer (red curve). After adding Exo I and III into the system, the solution showed a rapid color fading and became almost colorless within 30 min; also, a decreased absorption peak at 526 nm accompanied with another increasing absorption at 740 nm were observed, indicating the aggregation of AuNPs (green curve). The observation verified that Exo I and III could work well in Dnmt 1 assay buffer and effectively degrade the ABP DNA probe **1** on AuNPs, resulting in the aggregates of the dispersed AuNPs. The ABP DNA Probe **1** modified AuNP solution was incubated with 104 U/mL Dnmt 1 at 37 °C for 2 h followed by the digestion with Exo I and III at 37 °C for 30 min. As expected, in the presence of 104 U/mL Dnmt 1, no noticeable color change was observed and only slightly decreased absorption peak occurred after the Exo I and III digestion (blue curve). This implied that Dnmt1 could be covalently captured by ABP DNA probe **1** tethered on AuNPs and then prevented the double-stranded ABP DNA probe from digestion.

To validate the mechanism of the ABP-based colorimetric biosensor, control experiments were performed by incubating the control probe **1** which hybridized via Sequence **2** and Sequence **4** but 5-aza-dC was replaced by dC at hemimethylated CpG site modified AuNPs with Exo I and III in the presence of 104 U/mL Dnmt 1; a new absorption peak at 740 nm was obtained, and remarkable hypochromicity occurred at 528 nm (black curve). This revealed that, when there was no 5-aza-dCTP presence in duplex DNA hemimethylated CpG sites, Dnmt 1 failed to be covalently captured by duplex DNA tethered on AuNPs, so duplex DNA was degraded by Exo I and III inducing unstability of AuNPs in Dnmt1 assay buffer. Likewise, in another control experiment, where AuNPs modified by control probe **2** hybridized via Sequence **3** and Sequence **5** containing 5-aza-dC at nonmethylated CpG, sites were incubated with Exo I and III in the presence of 104 U/mL Dnmt 1 at 37 °C for 2 h; a new absorption peak at 740 nm was also obtained as well as a remarkable attenuation at 528 nm observed (pink curve). As shown in Figure 2, an obvious color change and remarkable spectral shift were observed. This demonstrates that, when no Dnmt 1 recognized sequence existed in duplex DNA, 5-aza-dCTP was also unable to covalently react with Dnmt 1 to form DNA−protein complex; thus, duplex DNA tethered on AuNPs would be digested by Exo I and III and resulted in aggregation of AuNPs. These controlled experiments demonstrated that Dnmt 1 could only be irreversibly covalently captured by double-stranded ABP DNA probe and protected ABP DNA probe tethered on AnNPs from being degraded by Exo I and III when both Dnmt 1-reactive nucleotide (5-aza-dCTP) and Dnmt 1-recognized sequence (hemimethylated CpG sites) were present, implying our colorimetric ABP-based colorimetric strategy could provide high selectivity and specificity for Dnmt1 activity and abundance detection. In addition, another controlled experiment was performed, 1 mM genistein (small-molecular inhibitor of Dnmt 1) was incubated with ABP DNA probe 1 decorated AuNPs containing 104 U/mL Dnmt1 prior to ExoI and III; the color of AuNPs and absorption peak changed distinctively (dark red curve). This assay might have potential use for inhibitor study and for screening of small molecules that inhibited the activity of Dnmt 1.

Characterization of ABP-Based Colorimetric Biosensor for Dnmt 1. More direct evidence of the biosensor mechanism was acquired through gel electrophoresis analysis, Figure 3. Double-stranded ABP DNA probe **1** gave a light band

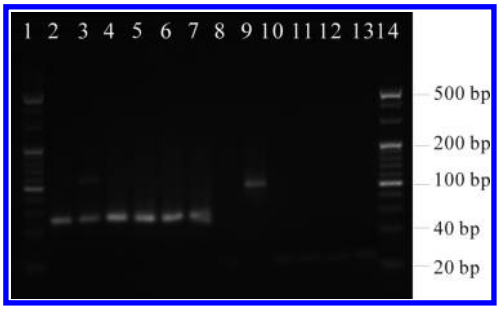

Figure 3. Gel electrophoresis image for assay of Dnmt 1 based on activity-based DNA. Lanes 1 and 14, DNA size marker; lanes 2 and 3, ABP DNA probe **1** before and after incubation with Dnmt 1; lanes 4 and 5, control probe **1** before and after incubation with Dnmt 1; lanes 6 and 7, control probe **2** before and after incubation with Dnmt 1; lanes 8, 10, and 12, treatment ABP DNA probe **1**, control probe **1** and **2** with Exo I and III; lanes 9, 11, and 13, ABP DNA probe **1**; control probes **2** and **3** incubated with Dnmt 1 followed by treatment with Exo I and III, respectively.

(lane 2). In the presence of 104 U/mL Dnmt 1, a new band with retarded mobility was observed in gel (lane 3), which was very different compared with lane 2, indicating the formation of covalent complex between Dnmt 1 and ABP DNA probe **1**. As controls, control probe **1** lacking 5-aza-dCTP at hemiethylated CpG sites gave two bright lands of the same mobility and intensity on the image (line 4 and 5) with or without incubation with Dnmt 1; similarly, control probe **2** containing 5-aza-dCTP at nonmethylated CpG sites also gave two bright lands of the same mobility and intensity (line 6 and 7) with or

dx.doi.org/10.1021/ac303575f | Anal. Chem. XXXX, XXX, XXX−XXX

without incubation with Dnmt 1. These results suggested that no complexes between the control probes and Dnmt 1 were formed and Dnmt 1 only bound selectively to duplex substrates with hemimethyleted CpG sites to form a covalent complex in the presence of 5-aza-dC. Interestingly, after using Exo I and III to sequentially treat with all the systems above, followed by deactivating Exo I and III and then adding Sequence **5**, only one bright band with obviously decreased migration shifts was observed (lane 9), and five bands with low molecular weights, which are from Sequence **5** added after deactivation of Exo I and III, were observed on the image (lanes 8, 10, 11, 12 and 13). This suggested that this retarded bright band was actually arising from Dnmt 1 covalent binding to double-stranded ABP DNA probe **1**, and the formation of covalent bond between Dnmt 1 and ABP DNA probe **1** indeed protected ABP DNA probe from degradation by Exo I and III.

To further verify the mechanism of our strategy, dynamic light scattering (DLS) analysis was performed to interrogate the AuNP aggregates mediated by Dnmt 1 covalent binding and Exo I and III digestion. As shown in Figure 4, the average hydrodynamic diameter of ABP DNA probe **1** modified AuNPs was ~35.7 nm. After Exo I and III degradation, the size of the AuNPs increased to ~1.2 μm. This indicated that the ABP DNA probe **1** on AuNPs was digested by Exo I and III. When adding Dnmt 1 into the ABP DNA probe **1** modified AuNP system incubated for 2 h before introducing Exo I and III for digestion, the size of AuNPs only slightly increased to ~61.2 nm, a size merely slightly bigger than that of ABP DNA probe **1** modified AuNPs. This conformed that the covalent binding between Dnmt 1 and ABP DNA probe **1** prevented duplex DNA from degradation by Exo I and III, thus protecting ABP DNA probe modified AuNPs against aggregation. As controls, incubating different sequence control probes containing only hemimethylated CpGs sites or only 5-aza-dC on non-methylated CpG sites, respectively, with Dnmt 1 and then following with the addition of Exo I and III, the size of AuNPs increased to ~1.23 and ~1.18 μm. This further verified that no covalent complexes between Dnmt 1 and control probes on AuNPs formed, showing that Dnmt 1 was selectively binded to duplex structures with hemimethylated sites to form a covalent complex with the additional present 5-aza-dCTP.

A transmission electron microscopy (TEM) investigation was performed to study the aggregation behavior of AuNPs as other evidence for further verifying the mechanism of the assay. As shown in Figure S1 (Supporting Information), in the presence of Dnmt 1, the TEM image of the ABP DNA probe **1** modified AuNPs after digestion by Exo I and III showed dispersed nanoparticles. In contrast, in absence of Dnmt 1, the digestion of the ABP DNA probe **1** modified AuNPs by Exo I and III gave large aggregates of nanoparticles. This confirmed again that the formation of covalent bond between Dnmt1 and ABP DNA probe **1** could prevent Exo I and III from digesting duplex DNA on AuNPs.

Quantitative Activity Detection of Dnmt 1 Using ABP-Based Colorimetric Biosensor. The ability of the colorimetric biosensor for quantitative detection of Dnmt 1 was investigated. The ABP DNA probe **1** which contained a 5′-aza-dC at hemimethylated CpG site was obtained via hybridization of Sequence **3** tethered on AuNPs and DNA Sequence **2**. A series of samples containing different Dnmt 1 concentrations were incubated with ABP DNA probe **1** modified AuNPs in the presence of 80 μM SAM at 37 °C for 2 h, and then, Exo I and III were added and incubated for another 30 min. Figure 5A shows the photograph of the activity-based DNA-gold nanoparticle probe after the digestion. It was observed that, with the decreasing Dnmt 1 concentration from 104 to 0 U/mL, the colors of AuNP solution spans red to blue−gray. This suggested that the presence of Dnmt 1 could prevent Exo I and III degrading ABP DNA probe **1** on AuNPs. These visual observations were consistent with the absorption spectral measurements. Figure 5B depicts the absorption spectra of the ABP DNA probe **1** modified AuNP solution after Exo I and III digestion in the presence of different concentrations of Dnmt 1. It was clear that with decreased Dnmt 1 concentration, the absorbance at 526 nm became broadened and decreased, accompanied with the appearance of a new absorbance peak at 740 nm. The peak intensity of absorbance at 526 nm versus Dnmt 1 concentrations showed a linear correlation with Dnmt 1 concentration range from 2 to 32 U/mL, as shown in Figure 5C. The detection limit was estimated to be 0.5 U/mL

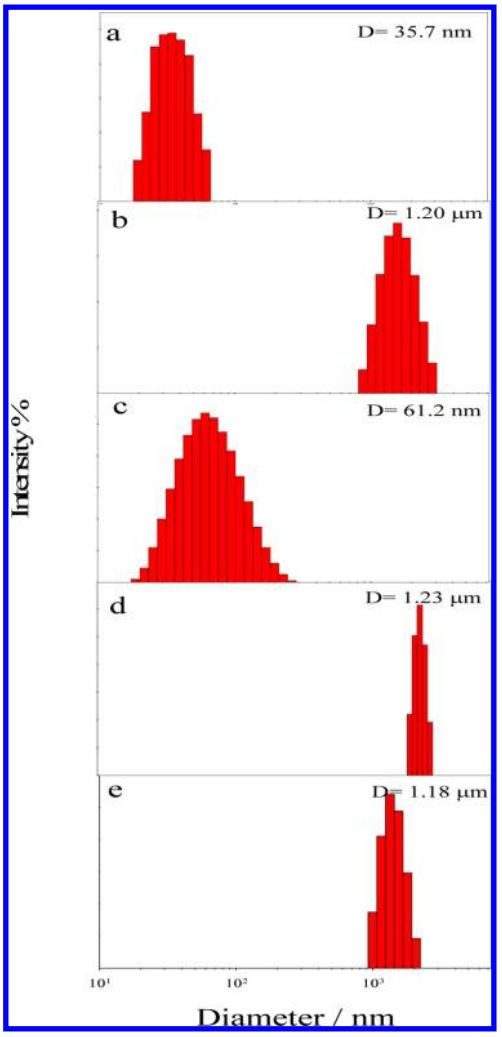

Figure 4. Hydrodynamic sizes of AuNPs determined by DLS analysis: (a) ABP DNA probe **1** modified AuNPs before digestion by 0.4 U/μL Exo I and 2 U/μL Exo III; (b) ABP DNA probe **1** modified AuNPs after digestion by 0.4 U/μL Exo I and 2 U/μL Exo III; (c) adding 104 U/mL Dnmt 1 into ABP DNA probe **1** modified AuNP system followed by digestion with 0.4 U/μL Exo I and 2 U/μL Exo III; (d) adding 104 U/mL Dnmt 1 into control probe **1** modified AuNP system followed by digestion with 0.4 U/μL Exo I and 2 U/μL Exo III; (e) adding 104 U Dnmt 1 into control probe **2** modified AuNP system followed by digestion with 0.4 U/μL Exo I and 2 U/μL Exo III.

dx.doi.org/10.1021/ac303575f | *Anal. Chem.* XXXX, XXX, XXX−XXX

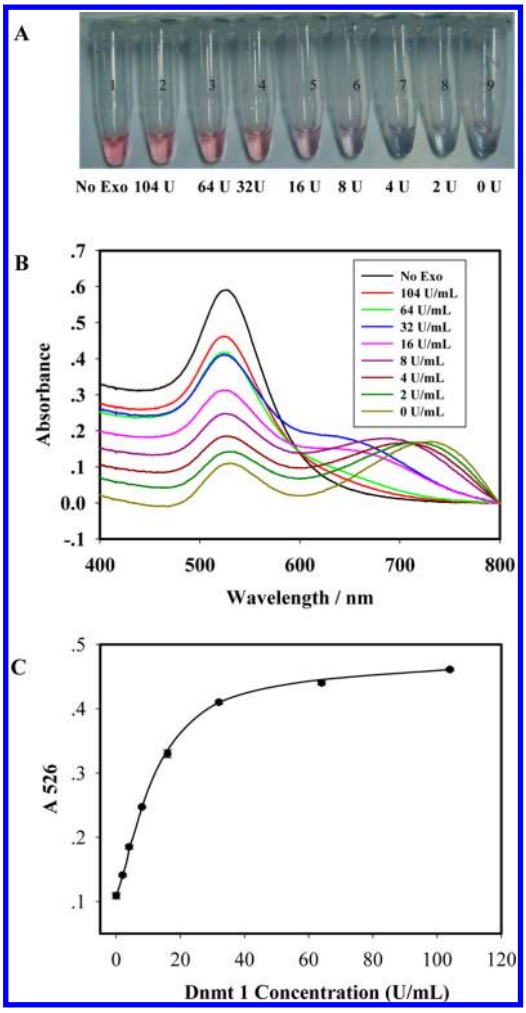

Figure 5. (A) Photographs of color change due to various Dnmt 1 concentrations. (B) Absorption spectral responses to various Dnmt 1 concentrations. (C) Measured absorbance (λ = 526 nm) versus Dnmt 1 concentrations.

according to the 3σ rule. This detection limit was comparable with those reported for coupled enzyme assays, ranging from 0.3 to 0.8 U/mL.[9,10] The developed strategy not only exhibited excellent reproducibility due to simple operations. The relative standard deviations (RSDs) of peak intensity of absorbance at 526 nm were 1.3%, 1.2%, 2.1%, and 1.8%, in four repetitive assays of 2, 8, 32, and 104 U/mL Dnmt 1. With the use of gold nanoparticle-based colorimetric assay, the developed strategy can create a convenient platform for visualized detection of enzyme activity and screening of ABPs for these enzymes with high sensitivity and selectivity. Therefore, we might conclude that the developed colorimetric biosensor held potential for a quantitative activity assay and abundance of the Dnmt 1 with desirable sensitivity and reproducibility.

Activity Assay of hOGG 1 Using ABP-Based Colorimetric Biosensor. In addition, the developed strategy was further validated using another DNA repairing enzyme hOGG 1. The double-stranded ABP DNA probe **2** which contained 8-oxo-dG was obtained via hybridization of Sequence **6** tethered on AuNPs and DNA Sequence **7**. As shown in Figure 6, before and after digesting by Exo I and III, ABP DNA probe **2** modified AuNPs incubated with 256 U/mL hOGG 1 for 90 min in the presence of 100 mM $NaBH_3CN$, there was no

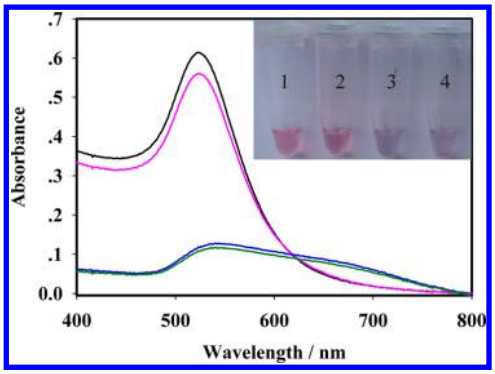

Figure 6. Absorption spectra obtained in assays of hOGG 1: ABP DNA probe **2** modified AuNPs before digestion by 0.4 U/μL Exo I and 2 U/μL Exo III (black, tube 1); ABP DNA probe **2** modified AuNPs after digestion by 0.4 U/μL Exo I and 2 U/μL Exo III (green, tube 3); adding 256 U/mL hOGG 1 ABP DNA probe **2** modified AuNP system followed by digestion with 0.4 U/μL Exo I and 2 U/μL Exo III (pink, tube 2); adding 256 U/mL hOGG 1 into control probe **3** modified AuNP system followed by digestion with 0.4 U/μL Exo I and 2 U/μL Exo III (blue, tube 4). The insets are the photographs for the corresponding systems.

appreciable change in the red color for the ABP DNA probe **2** modified AuNP solution. In contrast, no containing 8-hydroxy-2-deoxyguanosine (8-OHdG) control probe **3** via hybridization of Sequences **7** and **8** modified AuNPs incubated with 256 U/mL hOGG 1 under the same conditions followed by addition of Exo I and III; an obvious attenuation of the red color was observed for the solution of duplex DNA modified AuNPs. This indicated that hOGG 1 was selectively covalently trapped by double-stranded ABP DNA probe **2** containing 8-hydroxy-2-deoxyguanosine (8-OHdG) and protected the double-stranded ABP DNA probe **2** from degradation.

In addition, gel electrophoresis experiments were also taken to investigate the interaction between hOGG 1 and ABP DNA probe **2**. As shown in Figure S2 (Supporting Information), compared with the ABP DNA probe **2** (lane 2), when hOGG 1 existed, a bright band with obviously decreased migration shifts in the gel (lane 3) was observed. This gave immediate evidence of hOGG 1 binding ABP DNA probe **2**. As a control, incubating control probe **3** without 8-oxo-dG with hOGG 1 in the presence of $NaBH_3CN$, the same mobility bright band was observed (lane 4). This result revealed that hOGG 1 did not have unspecific binding control probe **3** without 8-oxo-dG. A further control experiment was performed by incubating ABP DNA probe **2** and hOGG 1 in the absence of $NaBH_3CN$, and in this case, a similar mobility band was obtained (lane 5), indicating that covalent complex formation could only occur in the presence of both hOGG 1 and $NaBH_3CN$. Interestingly, after using Exo I and III to treat the above systems, only DNA substrates covalently bound by hOGG 1 were remaining (lane 7), disclosing that hOGG 1 covalent binding to DNA substrates could prevent DNA substrates being digested by Exo I and III. As expected, the formation of covalent bond between enzymes and DNA substrates indeed prevented Exo I and III from digesting the DNA completely.

Activity-based DNA-gold nanoparticle probes for colorimetric activity assay of hOGG 1 were investigated by UV−vis absorption. As shown in Figure 7, it was observed that decreasing hOGG 1 concentrations resulted in a change in AuNP solution color from red to blue−gray the surface plasmon band gradually red-shifted and broadened, and the

dx.doi.org/10.1021/ac303575f | Anal. Chem. XXXX, XXX, XXX−XXX

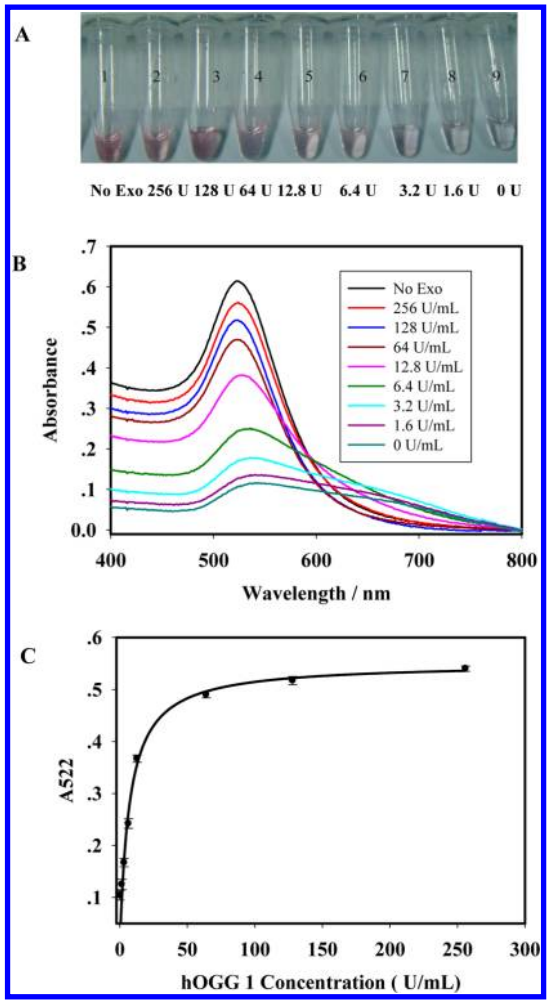

Figure 7. (A) Photographs of color change due to different hOGG 1 concentrations. (B) Absorption spectral responses to different hOGG 1 concentrations. (C) Measured absorbance (λ = 522 nm) versus hOGG 1 concentrations.

absorbance at 522 nm decreased, whereas that at 700 nm increased. By plotting the peak intensity of absorbance at 522 nm versus hOGG 1 concentrations, a work curve covering concentration range from 0 to 256 U/mL was obtained with linear response 0−64 U/mL. The detection limit was estimated to be 0.7 U/mL, in terms of the rule of 3 times standard deviation over the blank response. The RSDs of peak absorbance readings were 1.7%, 1.4%, 1.9%, and 1.5% in four repetitive assays of 1.6, 12.8, 64, and 256 U/mL hOGG 1. These findings implied that the developed strategy provides a sensitive and robust platform for activity assay of hOGG 1.

CONCLUSIONS

We have developed a novel ABP-based colorimetric biosensor strategy for detecting DNA methyltransferase/glycosylase activity with high sensitivity and selectivity. This design allowed a visual and homogeneous assay of the enzyme activity using the ABP−DNA probe. The biosensor had advantages over conventional assays, such as high specificity, speed, and convenience and reproducible detection due to homogeneous reactions. Compared with existing techniques for methyltransferase/glycosylase detection, this strategy offered improved selectivity and achieved the information about both abundance and activity of the enzymes because of mechanistically trapping of the enzyme by the ABPs. This method might hold great potential for activity assay of the enzymes in practical samples such as cell extracts. Additionally, it could be further extended to create a much more useful and convenient approach for visualized screening of ABPs for DNA modifying enzymes.

ASSOCIATED CONTENT

Supporting Information

Description of other experimental procedures and additional figures. This material is available free of charge via the Internet at http://pubs.acs.org.

AUTHOR INFORMATION

Corresponding Author

*E-mail: jianhuijiang@hnu.edu.cn. Tel.: 86-731-88821961. Fax: 86-731-88821916.

Notes

The authors declare no competing financial interest.

ACKNOWLEDGMENTS

This work was supported by NSFC (21025521, 21221003, 21205034, 21035001, 21190041), National Key Basic Research Program (2011CB911000), EU FP7-HEALTH-2010 Programme-GlycoHIT (260600), and NSF of Hunan Province (10JJ7002).

REFERENCES

(1) Jones, P. A.; Takai, D. *Science* **2001**, *293*, 1068−1070.
(2) Khanna, K. K.; Jackson, S. P. *Nat. Genet.* **2001**, *27*, 247−254.
(3) Reik, W.; Dean, W.; Walter, J. *Science* **2001**, *29*, 1089−1093.
(4) Motoyama, N.; Naka, K. *Curr. Opin. Genet. Dev.* **2004**, *11*, 11−16.
(5) Esteller, M. *Nat. Rev. Genet.* **2007**, *8*, 286−298.
(6) Coppedè, F.; Migheli, F.; Ceravolo, R.; Bregant, E.; Rocchi, A.; Petrozzi, L.; Unti, E.; Lonigro, R.; Siciliano, G.; Migliore, L. *Toxicology* **2010**, *278*, 199−203.
(7) Jones, P. A.; Baylin, S. B. *Cell* **2007**, *128*, 683−692.
(8) Xiang, Y.; Lu, Y. *Anal. Chem.* **2012**, *84*, 9981−9987.
(9) Li, J.; Yan, H. F.; Wang, K. M.; Tan, W. H.; Zhou, X. W. *Anal. Chem.* **2007**, *79*, 1050−1056.
(10) Liu, T.; Zhao, J.; Zhang, D. M.; Li, G. X. *Anal. Chem.* **2010**, *82*, 229−233.
(11) Ye, Y.; Stivers, J. T. *Anal. Biochem.* **2010**, *401*, 168−172.
(12) Wang, M.; Xu, Z. N.; Chen, L. J.; Yin, H. S.; Ai, S. Y. *Anal. Chem.* **2012**, *84*, 9072−9078.
(13) Kurita, R. J.; Niwa, O. *Anal. Chem.* **2012**, *84*, 7533−7538.
(14) Heal, W. P.; Dang, T. H. T.; Tate, E. *Chem. Soc. Rev.* **2011**, *40*, 246−257.
(15) Barglow, K. T.; Cravatt, B. F. *Nat. Methods* **2007**, *4*, 822−827.
(16) Hermetter, H. S. A.; Birner-Gruenberger, R. *Amino Acids* **2006**, *30*, 333−350.
(17) Kattenhorn, L. M.; Korbel, G. A.; Kessler, B. M.; Spooner, E.; Ploegh, H. L. *Mol. Cell* **2005**, *19*, 547−557.
(18) Mosammaparast, N.; Shi, Y. *Annu. Rev. Biochem.* **2010**, *79*, 155−179.
(19) Barglow, K. T.; Cravatt, B. F. *Angew. Chem., Int. Ed.* **2006**, *45*, 7408−7411.
(20) Schermelleh, L.; Spada, F.; Easweran, H. P.; Zolghadr, K.; Margot, J. B.; Cardoso, M. C.; Leonhardt, H. *Nat. Methods* **2005**, *2*, 751−756.
(21) Shigdel, U. K.; He, C. *J. Am. Chem. Soc.* **2008**, *130*, 17634−17635.
(22) Wu, Z.; Zhen, Z.; Jiang, J. H.; Shen, G. L.; Yu, R. Q. *J. Am. Chem. Soc.* **2009**, *131*, 12326−12332.
(23) Wu, Z.; Wang, H. Q.; Guo, M.; Tang, L. J.; Yu, R. Q.; Jiang, J. H. *Anal. Chem.* **2011**, *83*, 3104−3111.
(24) Li, E. *Nat. Rev. Genet.* **2002**, *3*, 662−673.

(25) Friedberg, E. C.; Waller, G. C.; Siede, W.; Wood, R. D.; Schultz, R. A.; Ellenberger, T. *DNA Repair and Mutagenesis*; ASM Press: Washington, D.C., 2006.
(26) Crabar, K. C.; Freeman, R. G.; Hommer, M. B.; Natan, M. J. *Anal. Chem.* **1995**, *67*, 735−743.
(27) Rosi, N. L.; Giljohann, D. A.; Thaxton, C. S.; Lytton-Jean, A. K. R.; Han, M. S.; Mirkin, C. A. *Science* **2006**, *312*, 1027−1030.
(28) Li, J.; Chu, X.; Liu, Y.; Jiang, J. H.; He, Z.; Zhang, Z.; Shen, G.; Yu, R. Q. *Nucleic Acids Res.* **2005**, *33*, No. e168.
(29) Huang, C. C.; Chui, S. H.; Huang, Y. F.; Chang, H. T. *Anal. Chem.* **2007**, *79*, 4798−4804.
(30) Shen, W.; Deng, H.; Gao, Z. *J. Am. Chem. Soc.* **2012**, *134*, 14678−14681.
(31) Seferos, D. S.; Giljohann, D. A.; Hill, H. D.; Prigodich, A. E.; Mirkin, C. A. *J. Am. Chem. Soc.* **2007**, *129*, 15477−15479.

dx.doi.org/10.1021/ac303575f | *Anal. Chem.* XXXX, XXX, XXX−XXX